Microwave-mediated synthesis of iron-oxide nanoparticles for use in magnetic levitation cell cultures

Leticia Bonfim, Priscila de Queiroz Souza Passos, Karina de Oliveira Gonçalves, Lilia Coronato Courrol, Flavia Rodrigues de Oliveira Silv[illegible]l.

Applied Nanoscience

ISSN 2190-5509

Appl Nanosci
DOI 10.1007/s13204-019-00962-1

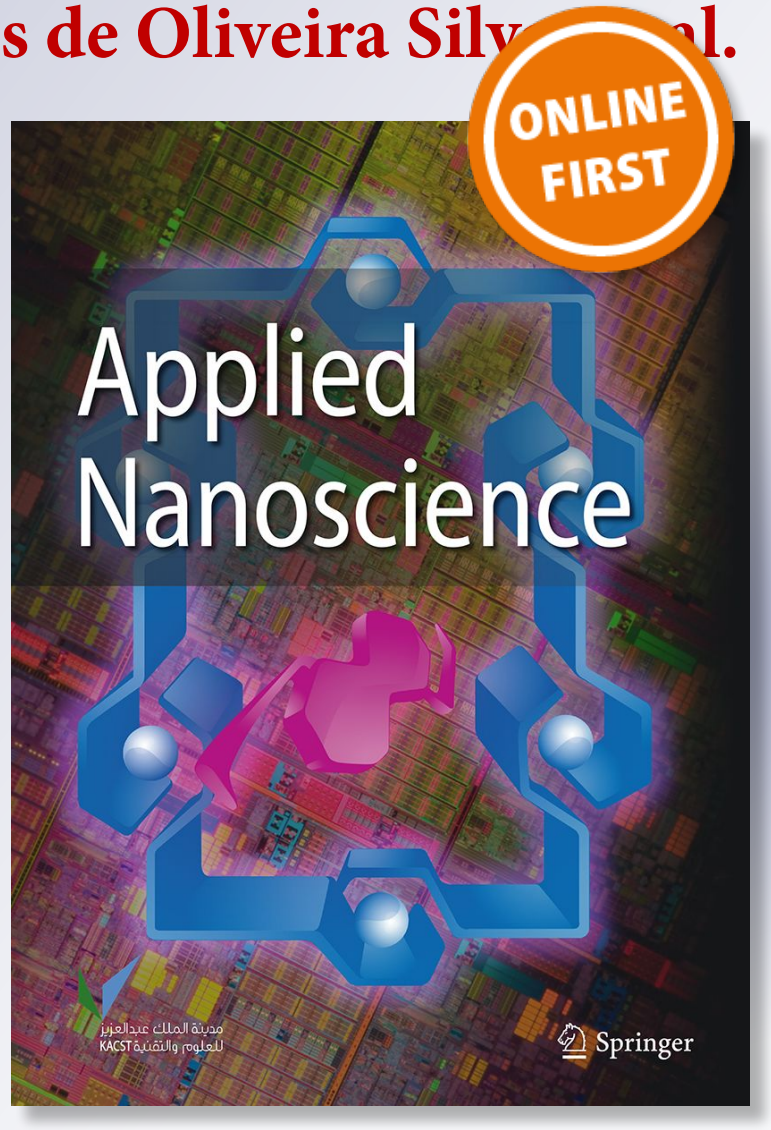

Springer

Applied Nanoscience
https://doi.org/10.1007/s13204-019-00962-1

ORIGINAL ARTICLE

Microwave-mediated synthesis of iron-oxide nanoparticles for use in magnetic levitation cell cultures

Leticia Bonfim[1] · Priscila de Queiroz Souza Passos[1] · Karina de Oliveira Gonçalves[2] · Lilia Coronato Courrol[2] · Flavia Rodrigues de Oliveira Silva[3] · Daniel Perez Vieira[1]

Received: 4 December 2018 / Accepted: 12 January 2019

Abstract
The use of three-dimensional cell cultures has been widely used for efficacy and/or toxicity testing of compounds. One of the most promising systems, based on magnetic levitation, is dependent on proper cell magnetization, achieved through adsorption of iron-oxide nanoparticles on cell membranes. These particles must bare not only significant responses to magnetic fields, but also a stable mechanism to attachment to cells. This work proposes a simple, one-pot synthesis method to produce magnetite nanoparticles, using a Fe^{2+} precursor associated with amino acids under microwave heating, and successive steps to confer positive charges to particles. X-ray diffraction could confirm Fe_3O_4 composition, and TEM analysis showed cubic-like crystallites with less than 50 nm. Zeta-potential experiments showed that particles remained positively charged (20.98 ± 0.28 mV) in physiological pH, suggesting ability to attach to (negatively charged) cell membranes, observed through optical microscopy. Iron colloid was found to be non-cytotoxic in concentrations up to 8% in cell culture media. Finally, human prostate cancer cells were cultured in 96-well plates using magnetic levitation and could be kept 8 days in culture. The results showed a feasible way to produce spheroids relying on magnetic levitation, using a newly described method of magnetic and cell adherent nanoparticle production.

Keywords PION · 3D cell culture · Magnetic levitation · Microwave synthesis · Nanotechnology

Introduction

Despite the large-scale use for the last 60 years (Eagle et al. 1958; Hirschberg 1958), there is already consistent scientific evidence that the two-dimensional arrangement prevents tumor cells from expressing their characteristics in a manner analogous to that found in the organism (Griffith and Swartz 2006). In order for these cell lines to behave more closely than those observed directly in vivo, three-dimensional cell interaction is required (Anton et al. 2015). In this way, the production and some level of encapsulation and interaction with extracellular matrix proteins are favored (Papusheva and Heisenberg 2010). Several methodologies capable of creating three-dimensional clusters of cells have been developed. The simplest form of cultivation of such clusters is the deposition of the cells on substrates whose electrical charge is non-adhesive or repellent to the cells (Kuwashima et al. 1993).

Several processes were developed to help researchers to grow tridimensional cellular aggregates in culture media. For example, cells can be encapsulated inside hydrogel microstructures (Han et al. 2013), or seeded on micropatterned surfaces (Wang et al. 2014; Qi et al. 2016). Other ways to produce spheroids in vitro can be based on rotating flasks or exogenous tumoral extracellular matrix (Engelbreth-Holm-Swarm) (Nath and Devi 2016), but simpler models, with no physical scaffolds, as used in in vitro bone repair models (Zhang et al. 2018), or with no requirement of special equipment, as on rotating flasks systems (Wuest et al.

✉ Daniel Perez Vieira
dpvieira@ipen.br

[1] Laboratório de Radiobiologia, Centro de Biotecnologia, Instituto de Pesquisas Energéticas e Nucleares, Av. Lineu Prestes 2242, São Paulo, São Paulo, Brazil

[2] Instituto de Ciências Ambientais, Químicas e Farmacêuticas, Departamento de Física, Universidade Federal de São Paulo, Rua Arthur Riedel 275, Diadema, São Paulo, Brazil

[3] Laboratório de Microscopia e Microanálise, Centro de Ciência e Tecnologia de Materiais, Instituto de Pesquisas Energéticas e Nucleares, Av. Lineu Prestes 2242, São Paulo, São Paulo, Brazil

Published online: 18 February 2019

2015) are desirable. Hanging drop culture is a technique with the promising results (Foty 2011; Shri et al. 2017), but requires some caution on manipulation of cultures.

Magnetic levitation cultures can produce spheroids up to 1 mm in diameter maintained for up to 4 weeks in culture (Lee and Hur 2014) without inducing a significant cytotoxicity in time scale and impractical physical dimensions in two-dimensional cultures. Its structure and maintenance ability in culture makes the spheroids candidates for long-term analyzes compared to the usual 4 or 24 h of exposure to test compounds (OECD TG 487 2014). The ability of a test compound to penetrate several cell layers can also be assessed (Jaganathan et al. 2014).

In this methodology, cells are kept floating in culture media under action of a magnetic field, usually due to paramagnetic iron-oxide nanoparticles (PION) internalized (Lee and Hur 2014) or associated with cell membranes (Souza et al. 2010). The latter approach allows particles to be trapped in extracellular matrix, forming a biological scaffold but responsible to magnetic fields.

Iron-oxide nanoparticles can be synthesized and functionalized interacting with cell membranes. Poly(L-lysine) coating is found to be well tolerable and non-toxic in tumoral (Wang et al. 2012; Ma et al. 2014) and non-tumoral (mesenquimal) cells (Sibov et al. 2012). Although amino acids like L-lysine can interact directly to surfaces of iron nanoparticles, a branching strategy can produce more stable colloids. A protocol described the L-lysine presence during coprecipitation of nanoparticles to, through interaction of carboxyl and Fe–O, allow the presence of amino groups on particle surface (Krishna et al. 2012). After this step, the researchers were able to coat particles with a solution of L-lysine, which when protonated, will render particles a positive surface charge. Glycine can be used also to functionalize particles surfaces with amino groups (Kumar et al. 2017).

The goal of the present work was to present a simple microwave-mediated, one-pot synthesis of paramagnetic iron-oxide nanoparticles properly functionalized with branched L-lysine to have a positive surface charge and thus, prone to adsorption on cell membranes. Cell cultures of human prostate adenocarcinoma were treated with iron colloid synthesized as described and was possible to produce spheroids through magnetic levitation.

Materials and methods

Cell culture

Human prostate cancer cells (LnCap) were cultured in incubator (37 °C, 5% CO_2) in 25 cm^2 flasks using 5 mL of RPMI 1640 media supplemented with fetal bovine serum (10%) and antibiotics (Pen/Streptomycin 10,000 U, Gibco). Medium was replaced every 48 h. After 70–80% confluence, cells were detached using trypsine/EDTA solution (0.25%) and subcultured.

Synthesis of iron nanoparticles

All solutions were readily prepared using deionized water deoxygenated through mild heating and vacuum (690 mmHg, 20 min). 32.5 mM of Iron(II) sulphate heptahydrated ($Fe_2SO_4{\cdot}7H_2O$, Sigma-Aldrich) was dissolved in deionized water prepared as described. 92.4 mM of Glycine (Sigma-Aldrich) was added and solution was slowly stirred for mixing. The pH of solution was corrected to 6.5 using NaOH 2M solution. The mixture was slowly poured into a borosilicate bottle and heated using a domestic microwave oven (max. power: 930 W) by 3 min and 1 min at time intercalated by mild agitation. In the presence of glycine as co-oxidizer, an amount of Fe^{2+} ions in solution could be oxidized to Fe^{3+}, and thus the ions were coprecipitated as iron-oxide crystals. The black precipitate was separated using a magnet and washed five times with deionized water prepared as above. After last wash, precipitate was resuspended in acetic acid (15 mL) and dispersed in an ultrasonic bath (5 min), and after this time, the iron oxide was separated using a magnet and acetic acid was discarded. L-Lysine (Sigma-Aldrich) was dissolved in water (1.5 mg/mL) and the pH of solution was adjusted to 11.0 using NaOH 2M. The nanoparticle suspensions were then dispersed again as described in the L-lysine solution. The nanoparticles were washed five times until pH 6.8–7.0 and finally suspended in 2 mL using deionized water. Suspensions were stored at 4 °C until use. Aliquots (100 µL) were diluted in ethanol, and particles were separated using magnets. Remaining pellets were dried overnight, and residues were weighted to determine particle concentration in colloids. Typically, 200–250 µg of nanoparticles were synthesized in each experiment. This approach was used to estimate amounts of iron nanoparticles before experiments.

Transmission electronic microscopy (TEM)

Nanoparticles were dispersed in isopropanol, dropped onto a carbon-coated copper grid, and analyzed by a JEM 2100 (JEOL) at Microscopy and Microanalysis Lab. of the Center of Material Science and Technology, IPEN/CNEN-SP.

Zeta-potential analysis

Suspensions were analyzed using a Litesizer 500 (Anton Paar GmbH, Austria). Omega cuvettes were filled with properly diluted dilutions of nanoparticles in water. A number of 1000 runs per sample were performed (200 V).

FTIR analysis

Fourier-transform infrared spectroscopy was performed in a Shimadzu IRPrestige-21 at Center of Instrumentation for Research and Teaching for Federal University of São Paulo (UNIFESP-Campus Diadema). The samples were prepared by pipetting 200 µL of the PION solutions, containing 25 µg of PIONS to be analyzed on a slide for microscopy and placed in an oven. After approximately 60 min, the solvent (water) had already evaporated and the procedure was repeated twice. The dried sample was extracted into potassium bromide (KBr) and pressed, obtaining a thin, translucent tablet, used for analysis. The obtained spectra were the results of 100 accumulated scans. Pure Glycine and L-lysine powders were used as spectral parameters to compare L-Lys-coated particles with its uncoated (only glycine) counterparts.

X-ray diffraction analysis

Suspensions were diluted in ethanol (9:1) and dried powders were analyzed using a Bruker D8 Advance 3 kW diffractometer, (Cu radiation tube, 250 mm goniometer, 40 kV, 30 mA) at Multiuser Center of the Center of Nuclear Fuel (IPEN/CNEN-SP). Spectra were analyzed using Qualx2 software (Altomare et al. 2015). The minimum FoM (figure of merit) allowed was 0.80. Peaks were compared to the compounds database of software to make assumptions between obtained crystal diffraction spectra versus those from known compounds. The full width at half maximum of peaks (FWHM) values were used to crystallite size calculations through Scherrer's calculation ($\lambda = 0.154056$, $K = 0.91$). Means of particle diameters were compared using unpaired Student's *t* test.

Adhesion to cell cultures

LnCap cells were trypsinized and cell suspensions in culture media (5 mL) received iron colloid (25 µg in 200 µL/2×10^6 cells and 4% of total volume of liquid in flasks). Cells were centrifuged (1500 rpm, 5 min) and resuspended in media for three consecutive times. Thereafter, cells were let to adhere and grow in flasks as described for 20 ± 2 h.

Prussian blue staining

LnCap cells were cultured in 25 cm^2 flasks in the presence of PION suspensions as described. After incubation time, media were removed, and cells were washed once in PBS (phosphate-buffered saline solution) (37 °C), and fixed subsequently with 100% methanol (20 min, RT). Methanol was removed, and cells were treated with 5 mL of a mixture of 2.5 mL of a solution of potassium ferrocyanide (2%, w/v in deionized water) and 2.5 mL of HCl 6%, by 30 min, RT. After color development, fixed cells were washed once in deionized water and imaged with a Nikon Eclipse Ts100.

Spheroid formation

Magnetic levitation plates were designed using a CAD software (SketchUp 2017, Trimble, Inc.) and printed using a 1.5 mm poly(l) lactic acid (PLA) filament in a 3D printer. All plates had 96 holes for fitting of neodymium cylindrical magnets (3×8.5 mm). These magnets have magnetic grade N35, with magnetic force at the surface of 5.9 kg, and 1.15 kg at 2 mm distance. Before use on cell culture, plates were sterilized by ethanol 70% wash and UV exposure (30 min) on sterile environment. Cells prepared as described, with nanoparticles attached to its membranes, were trypsinized and 5000 seeded per well (100 µL) in U-bottomed cell culture plates. Magnet plates were placed on top of wells, attracting cells to the center and to the top of liquid column. Cultures were kept in this way up to 8 days. Spheroid were imaged using microscope (Nikon 80i) at least each 24 h. Areas and perimeters were calculated through measurements using ImageJ 1.52 days (Schneider et al. 2012) after scale setting.

Cytotoxicity assays in 2D and 3D cultures

For analysis of toxicologic tolerance to nanoparticles, 5000 cells/well (100 µL) were seeded on in 96-well culture plates and cultured for 24 h as described. After this time, they were exposed to different concentrations of suspension (8, 4, 2, 1, 0.5, 0.25, 0.125, and 0.0063%, diluted in medium). Vehicle controls (VC) were prepared separating particles from liquid using a magnet for 10 min. Liquid-form suspensions were then diluted on medium (8, 4, and 1%). Latex extracts as positive controls (+) of 2-D cultures were prepared using a fragment (1 g) of a latex glove, sterilized by UV exposure on a sterile cabinet (30 min each side) Fragment was then immersed on 5 mL of culture medium in a conical tube and incubated for 24 h as described to cells. After this time, latex extracts were filter sterilized (0.22 µm) and used as is on cells on wells. Isotonic NaCl (0.9%) sterile solutions were prepared and diluted (5%) on media to perform negative (−) controls. After 24 h of incubation with particles, vehicle, and negative and positive controls, cells were washed once using PBS (37 °C) and received a solution of MTS (2 mg/mL in PBS) (CellTiter 96® AQueous Non-Radioactive Cell Proliferation Assay, Promega), PMS (0.92 mg/mL in PBS) (phenazine methosulfate, Sigma-Aldrich), and culture media in a proportion of 19:1:100, respectively. After incubation as described for 2 h, absorbance (λ 490 nm) of cultures was acquired in a Multiskan spectrophotometer (Thermo). Results were given as percentages of means of absorbance

values of cell controls (non-exposed cells). To test whether 3D cultures structured using the produced nanoparticles could be used on cytotoxicity testing, spheroids grown after 7 days in culture were exposed to NaCl as described (negative controls) or to dilutions of sodium dodecyl-sulphate (SDS) in medium (0.3125, 0.625, 1.25, 2.5, and 10 mM). After incubation as described for 24 h, viability was determined using the described MTS method.

Spheroid integrity and viability assessment through fluorescence imaging

After 7 days in culture, spheroids received acridine orange and ethidium bromide (100 µg/mL each) diluted in PBS. After incubation (20 min, RT), they were washed in PBS and imaged in a high-content analyzer (InCell Analyzer 2200, GE Lifesciences).

Results

Magnetic plate design and printing

After 3D printing, magnets were attached to PLA plates, as in Fig. 1a. Plates were placed on top of 96-well plates to compose individual magnetic fields (Fig. 1b). LnCap spheroids could be produced upon magnetic attraction of cells with adsorbed magnetite nanoparticles (Fig. 1c).

TEM

TEM imaging showed quasi-cubic particles, with dimensions of 50 nm or less, with high diversity of particle sizes (Fig. 2). No differences could be observed in shapes between particles obtained through syntheses with or without glycine, or even after L-lysine coating.

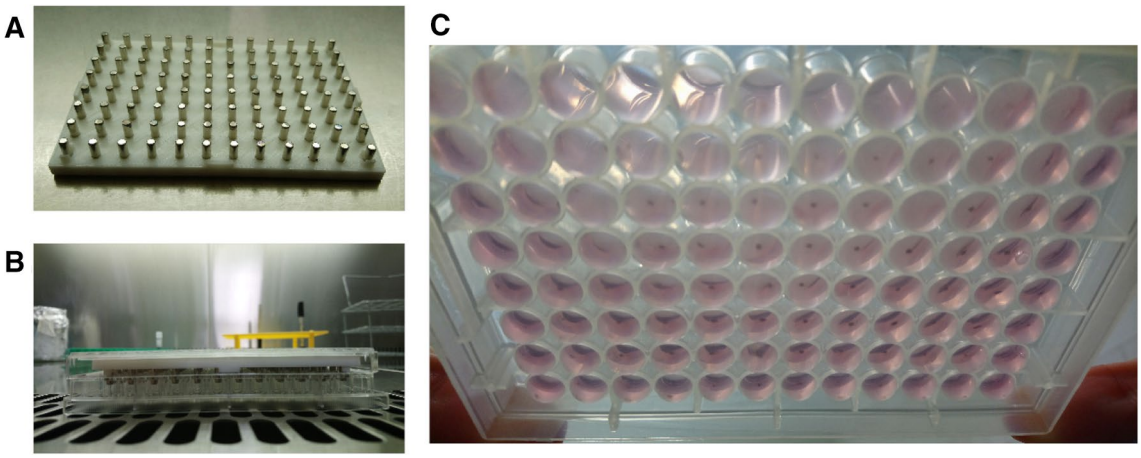

Fig. 1 Magnetic plate, printed in PLA matrix (**a**). Placement of magnets on top of 96-well cell culture plate (**b**). **c** LnCap spheroids could be observed during experiment. Picture showing spheroids after 8 days in culture

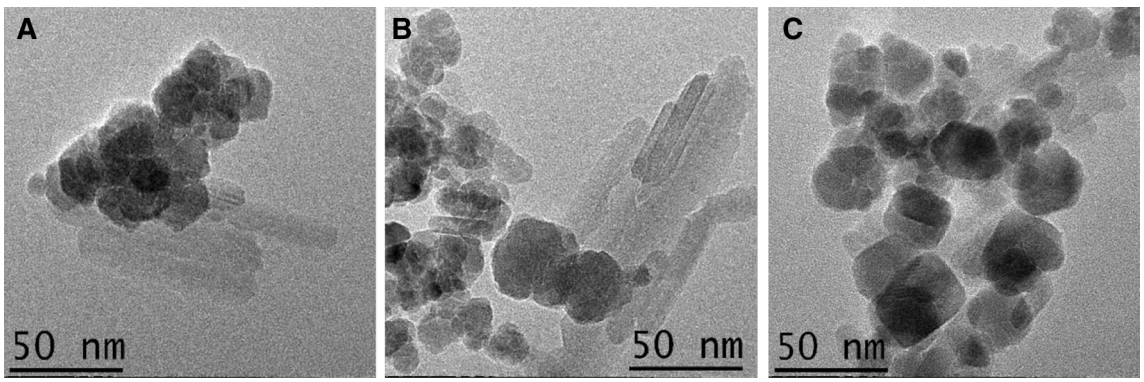

Fig. 2 Magnetite (Fe_3O_4) particles observed by TEM. PIONS synthesized without (**a**) or with (**b, c**) glycine. PIONS in **c** received also the L-lysine functionalization after synthesis

Zeta potential analysis

Data from suspensions obtained from three independent syntheses were used to analyze zeta potential of particles. The mean value was $+20.98 \pm 0.16$ mV in water, as shown in Fig. 3. Particles appeared to be positively-charged when synthesized with glycine and cover with L-Lys, in opposition to particles precipitated without glycine, which beared a much lower mean zeta potential value (-15.9 ± 0.98). Particles fabricated with glycine, but without lysine coating, presented similar mean zeta values ($+21.84 \pm 0.84$) from those coated with lysine.

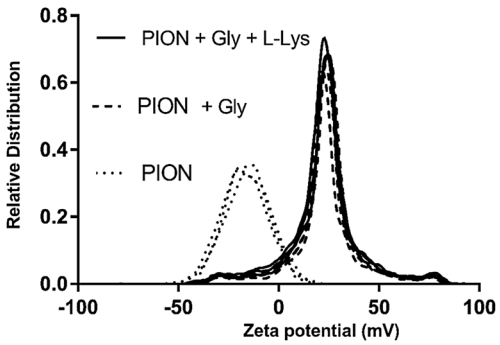

Fig. 3 Measurements of zeta potential of Fe_3O_4 bare particles (PION), Fe_3O_4 associated with glycine (PION + Gly), and with glycine and lysine (PION + Gly + L-Lys). Data from three independent syntheses

FTIR analysis

FTIR spectra were analyzed for the glycine and lysine amino acids alone and for iron nanoparticles with glycine (Fe + Gly) and with glycine and lysine (Fe + Gly + Lys). Glycine and lysine have the amine (NH_2) functional groups at ~ 3500 cm^{-1} and carboxyl (–COOH) at ~ 1600 cm^{-1}. These two groups are important for making bonds with metals through electrostatic interactions. In Fig. 4, the presence of the free amine NH_2 band (~ 3440 cm^{-1}) is observed for all samples, indicating that the amines are present on the surface of the iron nanoparticles. The C=O band of the carboxyl (~ 1615 cm^{-1}) present for glycine and lysine decreases in the spectra of the nanoparticles, suggesting that the binding with the metal ion is done with this functional group. They also exhibit absorption bands at 1550 cm^{-1} and 1430 cm^{-1} corresponding to the asymmetric and symmetrical stretches of the carboxylate.

X-ray diffraction analysis (XRD)

After background correction and narrowing search for accepting mainly Fe and O compounds, the software assigned distinct peaks, that could be found as characteristic of a monoclinic crystal structure compatible to magnetite (Fe_3O_4, Open Crystallography Database number: 00-153-2800). Peaks and diffraction planes are depicted in Fig. 5. No significant changes in diffraction spectra were found between particles synthesized with or without glycine. Using Scherrer's calculations, crystallites formed in the presence or absence of glycine were found

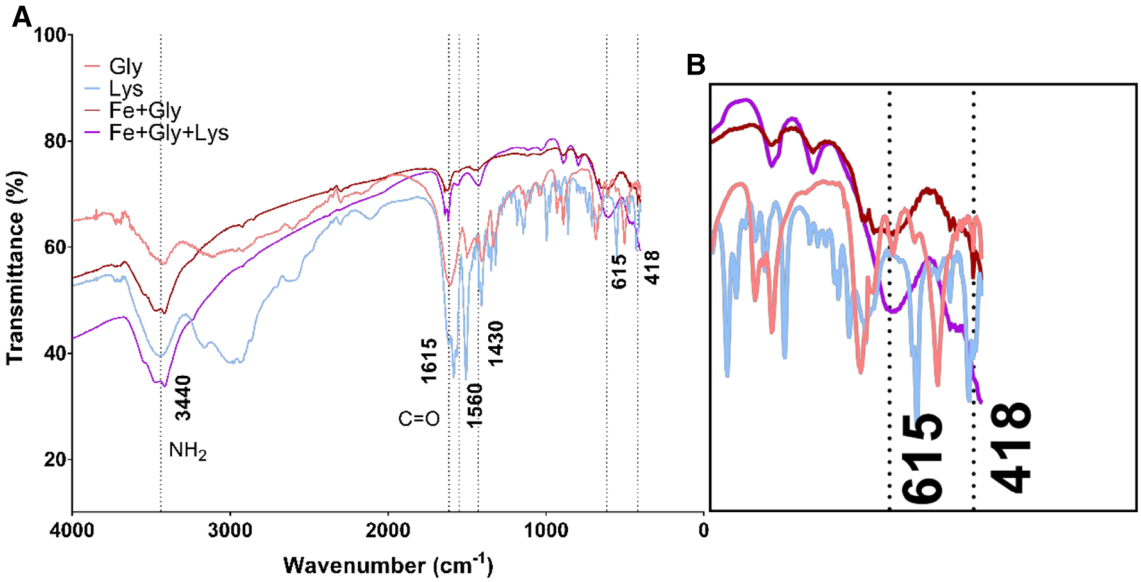

Fig. 4 **a** FTIR analysis of Fe_3O_4 nanoparticles synthesized with glycine (Fe + Gly), covered with lysine (Fe + Gly + Lys) and glycine and lysine spectra. **b** Same data; zoom in region to show the tensile (ν Fe–O) and deformation (δ Fe–O) bands

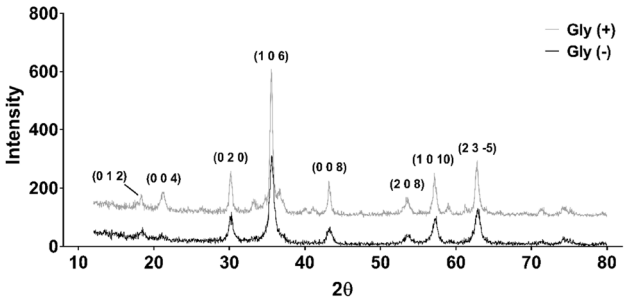

Fig. 5 X-ray diffraction spectra from crystallites synthesized with (gray) or without (black) glycine

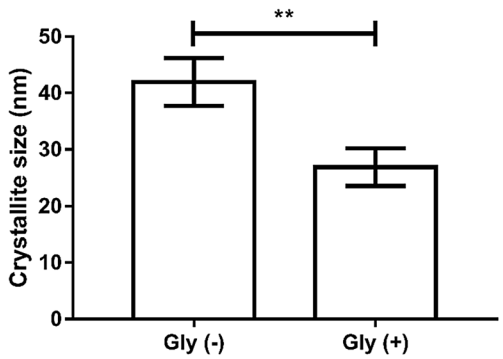

Fig. 6 Mean size of particles precipitated under the presence or absence of glycine obtained through Scherrer's calculation. (**): $p < 0.05$. Bars: SEM (standard error of means)

to have median values of 26.86 and 41.95 nm, respectively (Fig. 6).

Particle adhesion to cells

Fe_3O_4 paramagnetic nanoparticles suspension. Particles could be attracted to magnets (a). After centrifuge steps, cells appeared as a darkened pellet, with some turbidity remaining on media (Fig. 7b). As described, cells were kept 20 ± 2 h inside incubator, and showed a brown-colored contour (Fig. 7d), a signal considered typical upon iron-oxide accumulation. Not exposed cells (Fig. 7c) are shown for comparison.

Prussian blue staining showed nanoparticle aggregates around cell membranes. In Fig. 8, depicted images representing usual aspects of PION accumulation around cells.

To help visualization of the location of particles on cells, cultures were developed on coverslips exposing LnCap cells to PIONS as described, and seeding 50,000 viable cells/coverslip. After 24 h in culture, coverslips were washed with PBS and fixed using methanol as in Prussian blue assay. After fixation, coverslips were mounted on slides using a drop of PBS and imaged in a Nikon 80i optical microscope, with an immersion oil objective (100×). Aspect of cells is shown in Fig. 9.

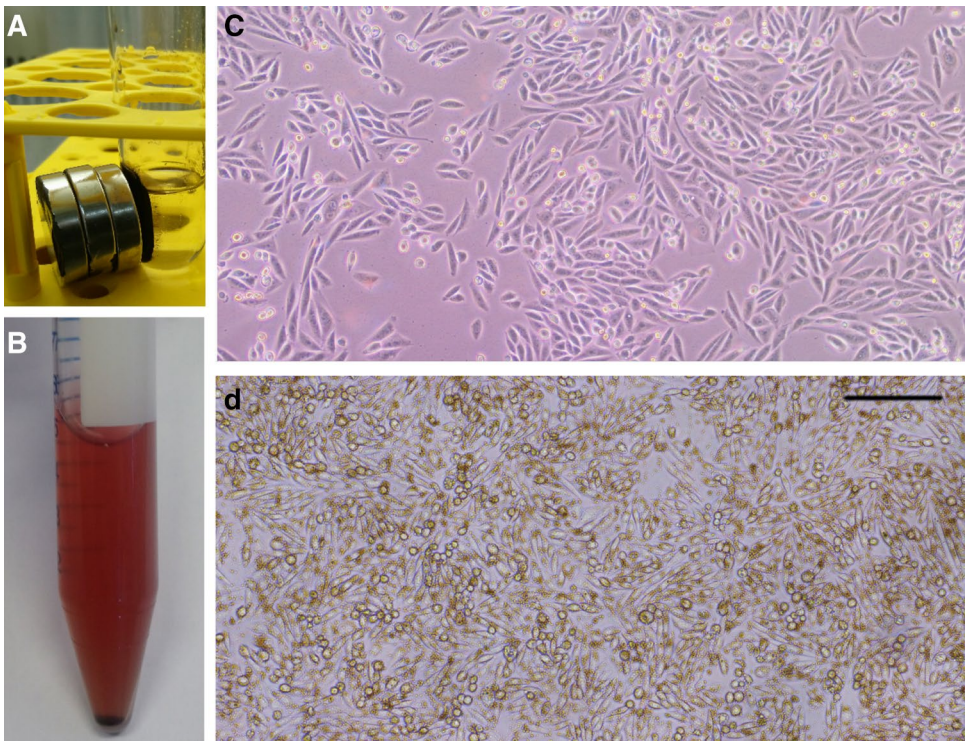

Fig. 7 **a** Attraction of Fe_3O_4 nanoparticles to a neodymium magnet. **b** LnCap cell pellet bearing darkened color, indicating association with particles. **c** LnCap control culture. **d** Visual aspect of LnCap cell culture exposed 24 h to Fe_3O_4 nanoparticles suspension. Magnification: ×10. Bar: 100 µm

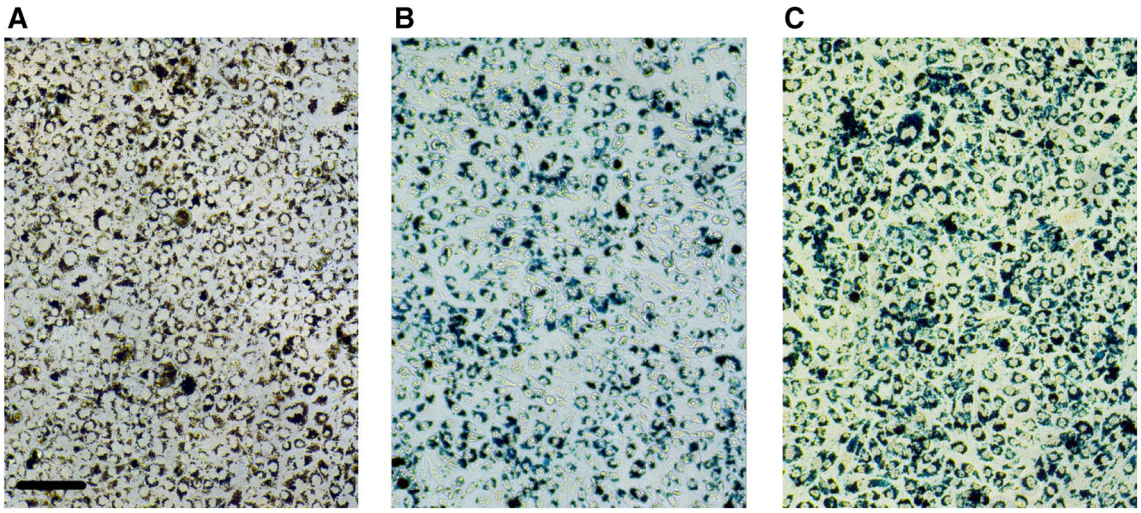

Fig. 8 Aspect of LnCap cultures after 24 h of exposure to 125 (**a, c**) or 62.5 µg/mL (**b**) of PION suspensions. **a** Usual aspect of PION's adsorbed in cell membranes. **b, c** Aspect of PIONS after Prussian blue staining. Magnification: ×10. Bar: 100 µm

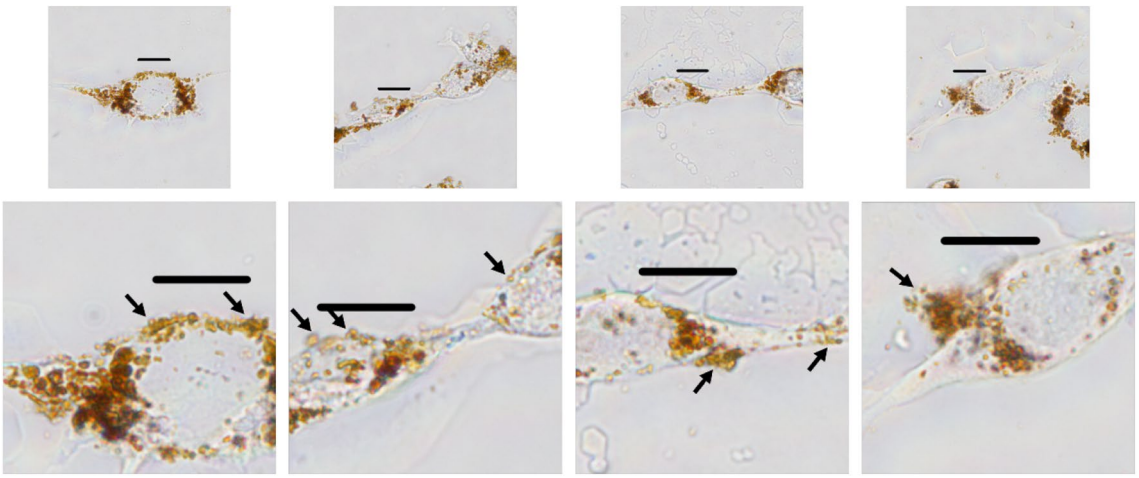

Fig. 9 LnCap cells bearing PION aggregates on surface of membranes (arrows). Magnification: ×100. Bars: 10 µm

Spheroid formation

Cell aggregates were observed from 1st to 8th day of experiment. At days 2nd and 3rd, areas of cell aggregates reached its maximum values during experiment. After 4th day of culture, values of areas started to decline until the end of experiment, and aggregates assumed a more spheric shape, in contrast to a previous configuration that resembled sheet-like structures (Fig. 10).

Cytotoxicity assays in 2D- and 3D cultures

To assess whether the synthesized iron colloid could induce cytotoxicity, LnCap cells were seeded (5000 cells/well) and, after 24 h, exposed to different concentrations of Fe_3O_4 nanoparticle suspensions. As shown in Fig. 11, any used concentrations did not induced cytotoxicity on cells.

LnCap spheroids were used to cytotoxicity tests also using MTS reduction as parameter. After 8 days in culture, spheroids were exposed in quadruplicates to negative and positive controls, as used in analysis of 2D cultures, and to increasing concentrations of SDS, a well-known toxic compound, as depicted in Fig. 12.

Spheroid integrity and viability assessment through fluorescence imaging

After 8 days in culture, cells were put in wells with PBS (pH 7.2) with a mixture of acridine orange and ethidium bromide. Two typical acquisitions are shown in Fig. 13. Using

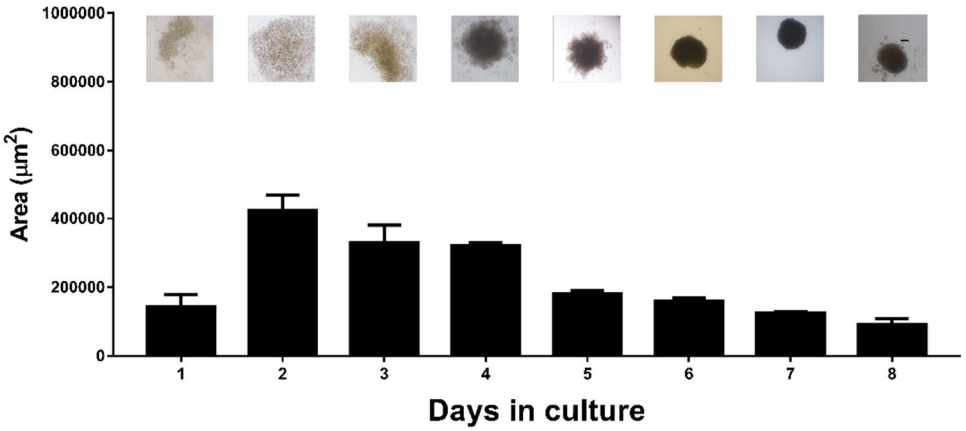

Fig. 10 Mean values of areas of cultured LnCap spheroids during the 8 days of experiment. Top: typical aspect of spheroids in each day of experiment. Bar inside picture of spheroid after 8 days in culture: 100 µm. Error bars: SEM (standard error of means)

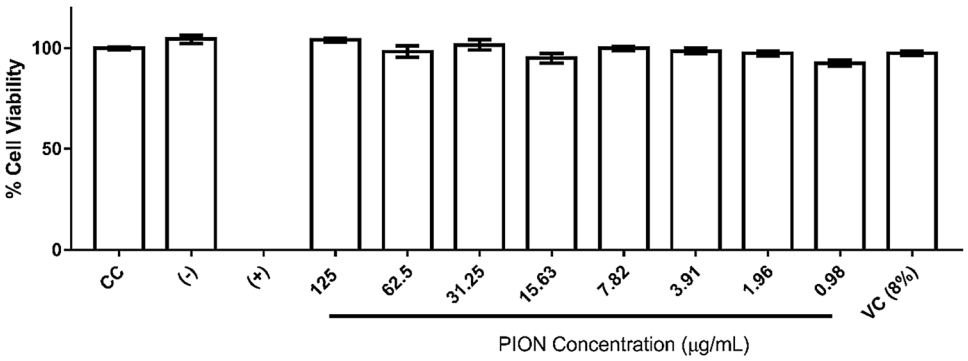

Fig. 11 Cytotoxicity assay of 2D LnCap cultures after 24 h of exposure to nanoparticles. *CC* control cells, *VC* vehicle controls (deionized water). (−) Negative (NaCl 0.9%) control. (+) Positive (latex extract) control. VC (8%): vehicle control, 8% of medium volume, corresponding to the volume of the higher PION concentration. Error bars: SEM (standard error of means)

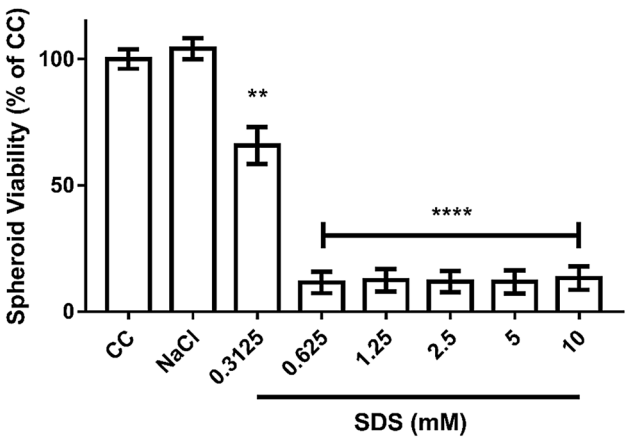

Fig. 12 MTS reduction tests, using LnCap (8 days of culture) spheroids obtained by magnetic levitation. *CC* control cells—spheroids cultured only with medium. (**): $p < 0.01$. (****): $p < 0.0001$. Error bars: SEM (standard error of means)

a regular cell culture plate, with bottom thickness around 1 mm, fluorescence appeared dimmed (a). Using an imaging plate, green fluorescence of acridine orange could be detected more brilliant, and a red-stained dead/unviable core could be observed, due to ethidium bromide incorporation (b).

Discussion

The paper replicated with success a cell culture process based on magnetic levitation already established and elsewhere described (Haisler et al. 2013; Tseng et al. 2015; Adine et al. 2018). As on that model, paramagnetic iron-oxide nanoparticles were designed to be adsorbed on cell membranes, instead of being internalized in the cell via membrane invagination, as reported by others when analyzing cell uptake of organic-coated (fibroin) microspheres (Lee and Hur 2014; Jeong et al. 2016). This approach can be prone in preventing nanoparticles form entering the cellular iron metabolism, which was related to cell physiology disruption, as in macrophages and in tumors (Legendre and Garcion 2015; Rojas et al. 2016).

The proposed colloid can be stated as a simplified version of the commercial product, which is based on an association with iron and gold nanoparticles (Souza et al. 2010). Nevertheless, the proposed system produced consistent cell spheroids using the conventional U-bottomed cell-cultured plates and an in-house printed magnet array, as shown in Fig. 1.

L-Lysine was added as a way of delivering positive charges to the particles, and to allow its adsorption to

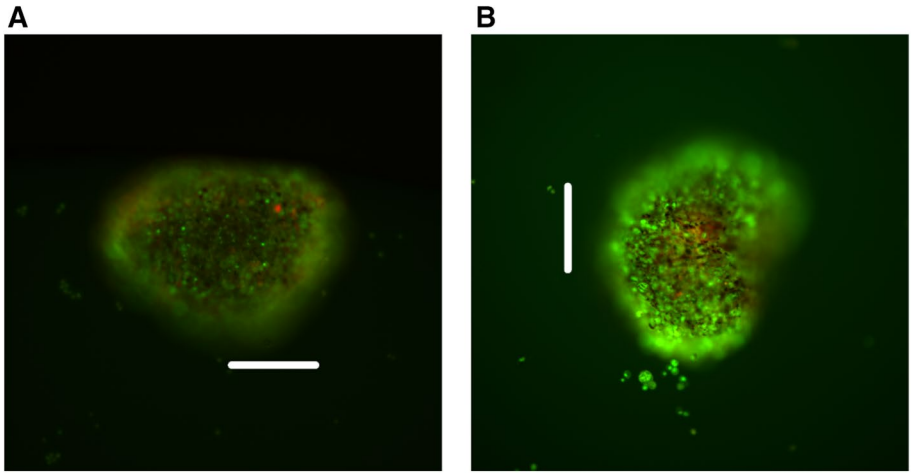

Fig. 13 Spheroids imaged using a regular cell culture plate (**a**) and imaging plate (**b**). Magnification: ×10. Bars: 200 µm. Green regions are related to acridine orange viability staining. Orange/red regions are related to ethidium bromide incorporation, and thus indicating cell death

the cell membranes, not as surfactant / dispersant, which would be inefficient given the aqueous solvent in which the PIONS were dispersed. Surface charges are a conditional factor for dispersion, but it was considered that the zeta-potential values (around + 20 mV) would not be sufficient to produce monodispersion.

Since the first publications using it (Massart et al. 1995), the co-precipitation method and its variations are widely used for the production of paramagnetic nanoparticles (Laurent et al. 2008; Wu et al. 2008, 2015). Cubic (or quasi-cubic) iron-oxide nanoparticles, as those obtained in this work, were produced by others (Predoi 2007; Cheraghipour et al. 2012; Hasany et al. 2013; Mascolo et al. 2013; Riaz et al. 2014; Hashem et al. 2018), consistent with its crystallographic system (Teja and Koh 2009).

Citrate ions are commonly used as surfactant in iron-oxide nanoparticles synthesis (Babic et al. 2008; Cheraghipour et al. 2012; PSoares et al. 2015; Shrestha et al. 2016). In addition to guaranteeing the dispersion of the particles giving them surface charge, the citrate ions are an important chelator that can modulate the particle size by inhibition of crystal nucleation and surface hydrolysis (Bee et al. 1995), through the interaction of the carboxylates with the Fe ions (Sahoo et al. 2005). The work intended to use glycine as chelator, using its carboxyl radical adsorbed to nanoparticles surface, and thus exposing its amine groups to medium. Comparison of mean crystallite diameters calculated through Scherrer's formulae showed that glycine presence reduced significantly the size of nanoparticles. The tensile (ν Fe–O) and deformation (δ Fe–O) bands of the Fe–O bond occur in the region between 400 and 650 cm^{-1}, and can be assigned to magnetite (Gotić and Musić 2007). In the FTIR spectrum of iron nanoparticles (Fe + Gly and Fe + Gly + Lys), the bands are observed at 615 cm^{-1} and 400 cm^{-1}, which are associated with the octahedral and tetrahedral sites of the spinel structure, which indicates the interaction of iron with the oxygen of the carboxyl group. In addition, glycine presence did not seem to alter significantly the crystalline structure, or the iron oxide produced during precipitation, as showed by XRD studies, which also confirmed the production of Fe_3O_4 after peak profile comparison using software. Microwave synthesis was found to be a suitable quick one-pot synthesis to produce considerable amounts of Fe_3O_4 to be used on magnetic levitation of cell cultures.

After protonation through ultrasonic treatment on presence of acetic acid, glycine amine groups (supposedly exposed to external surface of particles) were able to interact with ionized carboxyl groups from L-lysine, making possible the formation of stable bonds between the L-lysine chains and the nanoparticles. Bare iron nanoparticles, synthesized without glycine, showed negative zeta-potential values, and thus, not suitable to be adsorbed onto cell membranes. Colloids synthesized with glycine but with no L-lysine coating were not able to adhere in cells (data not shown), despite its positive (and comparable to L-lysine coated particles) zeta potential value. Other authors were able to detect cell uptake of glycine and lysine PION's (Wu et al. 2014), but this work was not able to show this phenomenon.

Glycine is a non-charged aminoacid and, due to its isoelectric point (pI = 6), does not have significant charge under physiological pH. Lysine is a cationic amino acid, which can show protonation in the R group at pH values higher than physiological aminoacid (pKa = 10.5, pI = 9.74). Thus, it can bear a positive charge in cell culture conditions, which can be responsible to cell attachment. There is some evidence that lysine can bind strongly to phospholipids than glycine (Porasso et al. 2015), what can explain at least to a limited extent the successful binding of lysine-coated PIONS instead of glycine-coated.

Glycine supplementation was shown to be effective on reducing particle size and to enable L-lysine attachment to particle surfaces, as detected by the FTIR analysis. In the present experiments, Prussian blue staining was

unequivocal showing PION accumulation externally to cells. The work did not perform any experiment to determine whether PIONS could be internalized by cells, but Prussian blue staining and 100× magnification, indicating external localization, and no occurrence of cytotoxicity in concentrations up to 125 µg/mL could be taken as a reliable indication that no uptake and no deleterious interactions with membranes were possible in experiments.

After 6 days in culture, spheroids retained a relatively spherical aspect, and appeared opaque to light. This work did not develop any study to determine the presence of extracellular matrix proteins, but, at this day, the bodies appeared compact and remained solid even after magnet removal, indicating strong cohesion. Another study obtained similar results, stable and knitted LnCap spheroids, using 7000 cells growing for 5 days (Edmondson et al. 2016).

Spheroids obtained using the present PIONS as magnetic scaffold could be tested for SDS-induced cytotoxicity using a standard MTS reduction test, and could be imaged through conventional (inverted) microscopy. Determinations of spheroid diameters and perimeters using digital acquisitions were shown to be relatively feasible, despite its acquisition time (approx. 2 h for 80 spheroids, data not shown). If available, the proposed PION suspension is completely compatible with imaging in high content screening (HCS) platforms using fluorescence analysis, as commercially available product. The purpose of the comparison was to show that it can be possible to imaging cell spheroids using the incorporation of this fluorescent probes even in ordinary culture plates despite the use of imaging plates led to a great increase of signal. The appearance of the center of spheroids colored in red or orange as an accumulation of ethidium bromide is consistent to internal necrotic areas due to the lack of proper nutrient and oxygen diffusion from medium to cells in the inner layers.

Conclusion

The work described a simple method to synthesize paramagnetic iron-oxide nanoparticles using glycine, with reduced the mean size of crystallites, as assessed by the XRD studies. Successive coating with L-lysine, bound to glycine-NH_2 groups, was sufficient to confer adherence of particles on cell membranes. Prostate cancer cell spheroids obtained by this method remained stable in culture for at least 8 days. Spheroids are similar to those obtained using commercially available products, with the same capabilities as test systems for cellular toxicity.

References

Adine C, Ng KK, Rungarunlert S et al (2018) Engineering innervated secretory epithelial organoids by magnetic three-dimensional bioprinting for stimulating epithelial growth in salivary glands. Biomaterials 180:52–66. https://doi.org/10.1016/j.biomaterials.2018.06.011

Altomare A, Corriero N, Cuocci C et al (2015) QUALX2.0: a qualitative phase analysis software using the freely available database POW-COD. J Appl Crystallogr 48:598–603. https://doi.org/10.1107/S1600576715002319

Anton D, Burckel H, Josset E, Noel G (2015) Three-dimensional cell culture: a breakthrough in vivo. Int J Mol Sci 16:5517–5527. https://doi.org/10.3390/ijms16035517

Babic M, Horák D, Trchová M et al (2008) Poly(L-lysine)-modified iron oxide nanoparticles for stem cell labeling. Bioconjug Chem 19:740–750. https://doi.org/10.1021/bc700410z

Bee A, Massart R, Neveu S (1995) Synthesis of very fine maghemite particles. J Magn Magn Mater 149:6–9. https://doi.org/10.1016/0304-8853(95)00317-7

Cheraghipour E, Javadpour S, Mehdizadeh AR (2012) Citrate capped superparamagnetic iron oxide nanoparticles used for hyperthermia therapy. J Biomed Sci Eng 05:715–719. https://doi.org/10.4236/jbise.2012.512089

Eagle H, Foley GE, Foley E (1958) Cytotoxicity in human cell cultures as a primary screen for the detection of anti-tumor agents cytotoxicity in human cell cultures as a primary screen for the detection of anti-tumor agents. Cancer Res 9:1017–1025

Edmondson R, Adcock AF, Yang L (2016) Influence of matrices on 3D-cultured prostate cancer cells' drug response and expression of drug-action associated proteins. PLoS One 11:1–23. https://doi.org/10.1371/journal.pone.0158116

Foty R (2011) A simple hanging drop cell culture protocol for generation of 3D spheroids. J Vis Exp 20:4–7. https://doi.org/10.3791/2720

Gotić M, Musić S (2007) Mössbauer, FT-IR and FE SEM investigation of iron oxides precipitated from $FeSO_4$ solutions. J Mol Struct 834–836:445–453. https://doi.org/10.1016/j.molstruc.2006.10.059

Griffith LG, Swartz MA (2006) Capturing complex 3D tissue physiology in vitro. Nat Rev Mol cell Biol 7:211–224. https://doi.org/10.1038/nrm1858

Haisler WL, Timm DM, Gage JA et al (2013) Three-dimensional cell culturing by magnetic levitation. Nat Protoc 8:1940–1949. https://doi.org/10.1038/nprot.2013.125

Han YL, Yang Y, Liu S et al (2013) Directed self-assembly of microscale hydrogels by electrostatic interaction. Biofabrication. https://doi.org/10.1088/1758-5082/5/3/035004

Hasany F, Ahmed S, Rehman IJR A (2013) Systematic review of the preparation techniques of iron oxide magnetic nanoparticles. Nanosci Nanotechnol 2:148–158. https://doi.org/10.5923/j.nn.20120206.01

Hashem F, Nasr M, Ahmed Y (2018) Preparation and evaluation of iron oxide nanoparticles for treatment of iron deficiency anemia. Int J Pharm Pharm Sci 10:142. https://doi.org/10.22159/ijpps.2018v10i1.22686

Hirschberg E (1958) Tissue culture in cancer chemotherapy screening. Cancer Res 18:869–878. https://doi.org/10.1126/science.35.913.979

Jaganathan H, Gage J, Leonard F et al (2014) Three-dimensional in vitro co-culture model of breast tumor using magnetic levitation. Sci Rep 4:1–9. https://doi.org/10.1038/srep06468

Jeong YG, Lee JS, Shim JK, Hur W (2016) A scaffold-free surface culture of B16F10 murine melanoma cells based on magnetic levitation. Cytotechnology 68:2323–2334. https://doi.org/10.1007/s10616-016-0026-7

Krishna R, Titus E, Krishna R et al (2012) Wet-chemical green synthesis of L-lysine amino acid stabilized biocompatible iron-oxide magnetic nanoparticles. J Nanosci Nanotechnol 12:6645–6651. https://doi.org/10.1166/jnn.2012.4571

Kumar R, Pandey K, Sahoo GC et al (2017) Development of high efficacy peptide coated iron oxide nanoparticles encapsulated amphotericin B drug delivery system against visceral leishmaniasis. Mater Sci Eng C 75:1465–1471. https://doi.org/10.1016/j.msec.2017.02.145

Kuwashima Y, Yamada T, Saio M, Takami T (1993) Formation and growth of multicellular spheroids in media containing low concentrations of agarose. Cancer Lett 71:31–33

Laurent S, Forge D, Port M et al (2008) Magnetic iron oxide nanoparticles: synthesis, stabilization, vectorization, physicochemical characterizations, and biological applications. Chem Rev 108:2064–2110. https://doi.org/10.1021/Cr900197g

Lee JH, Hur W (2014) Scaffold-free formation of a millimeter-scale multicellular spheroid with an internal cavity from magnetically levitated 3T3 cells that ingested iron oxide-containing microspheres. Biotechnol Bioeng 111:1038–1047. https://doi.org/10.1002/bit.25156

Legendre C, Garcion E (2015) Iron metabolism: a double-edged sword in the resistance of glioblastoma to therapies. Trends Endocrinol Metab 26:322–331. https://doi.org/10.1016/j.tem.2015.03.008

Ma YH, Peng HY, Yang RX, Ni F (2014) Preparation of lysine-coated magnetic Fe_2O_3 nanoparticles and influence on viability of a 549 lung cancer cells. Asian Pacific J Cancer Prev 15:8981–8985. https://doi.org/10.7314/APJCP.2014.15.20.8981

Mascolo MC, Pei Y, Ring TA (2013) Room Temperature co-precipitation synthesis of magnetite nanoparticles in a large pH window with different bases. Materials (Basel) 6:5549–5567. https://doi.org/10.3390/ma6125549

Massart R, Dubois E, Cabuil V, Hasmonay E (1995) Preparation and properties of monodisperse magnetic fluids. J Magn Magn Mater 149:1–5. https://doi.org/10.1016/0304-8853(95)00316-9

Nath S, Devi GR (2016) Three-dimensional culture systems in cancer research: focus on tumor spheroid model. Pharmacol Ther 163:94–108. https://doi.org/10.1016/j.pharmthera.2016.03.013

OECD TG 487 (2014) OECD Guideline for in vitro mammalian cell Micronucleus Test. n. September, p 1–26. Available at: https://ntp.niehs.nih.gov/iccvam/suppdocs/feddocs/oecd/oecd-tg487-2014-508.pdf.

Papusheva E, Heisenberg C-P (2010) Spatial organization of adhesion: force-dependent regulation and function in tissue morphogenesis. EMBO J 29:2753–2768. https://doi.org/10.1038/emboj.2010.182

Porasso RD, Ale NM, Ciocco Aloia F et al (2015) Interaction of glycine, lysine, proline and histidine with dipalmitoylphosphatidylcholine lipid bilayers: a theoretical and experimental study. RSC Adv 5:43537–43546. https://doi.org/10.1039/c5ra03236a

Predoi D (2007) A study on iron oxide nanoparticles coated with dextrin obtained by co precipitation. Dig J Nanomater Biostruct 2:169–173

Qi H, Huang G, Han YL et al (2016) In vitro spatially organizing the differentiation in individual multicellular stem cell aggregates. Crit Rev Biotechnol 36:20–31. https://doi.org/10.3109/07388551.2014.922917

Riaz S, Bashir M, Naseem S (2014) Iron oxide nanoparticles prepared by modified co-precipitation method. IEEE Trans Magn. https://doi.org/10.1109/TMAG.2013.2277614

Rojas JM, Sanz-Ortega L, Mulens-Arias V et al (2016) Superparamagnetic iron oxide nanoparticle uptake alters M2 macrophage phenotype, iron metabolism, migration and invasion. Nanomed Nanotechnol Biol Med 12:1127–1138. https://doi.org/10.1016/j.nano.2015.11.020

Sahoo Y, Goodarzi A, Swihart MT et al (2005) Aqueous ferrofluid of magnetite nanoparticles: fluorescence labeling and magnetophoretic control. J Phys Chem B 109:3879–3885. https://doi.org/10.1021/jp045402y

Schneider CA, Rasband WS, Eliceiri KW (2012) NIH Image to ImageJ: 25 years of image analysis. Nat Methods 9:671–675. https://doi.org/10.1038/nmeth.2089

Shrestha S, Jiang P, Sousa MH et al (2016) Citrate-capped iron oxide nanoparticles impair the osteogenic differentiation potential of rat mesenchymal stem cells. J Mater Chem B 4:245–256. https://doi.org/10.1039/C5TB02007G

Shri M, Agrawal H, Rani P et al (2017) Hanging drop, a best three-dimensional (3D) culture method for primary buffalo and sheep hepatocytes. Sci Rep 7:1–13. https://doi.org/10.1038/s41598-017-01355-6

Sibov TT, Miyaki LAM, Mamani JB et al (2012) Evaluation of umbilical cord mesenchymal stem cell labeling with superparamagnetic iron oxide nanoparticles coated with dextran and complexed with poly-L-lysine. Einstein (Sao Paulo) 10:180–188. https://doi.org/10.1590/s1679-45082012000200011

Soares IP, Lochte P, Echeverria F C, et al (2015) Thermal and magnetic properties of iron oxide colloids: influence of surfactants. Nanotechnology 26:425704. https://doi.org/10.1088/0957-4484/26/42/425704

Souza GR, Molina JR, Raphael RM et al (2010) Three-dimensional tissue culture based on magnetic cell levitation. Nat Nanotechnol 5:291–296. https://doi.org/10.1038/nnano.2010.23

Teja AS, Koh PY (2009) Synthesis, properties, and applications of magnetic iron oxide nanoparticles. Prog Cryst Growth Charact Mater 55:22–45. https://doi.org/10.1016/j.pcrysgrow.2008.08.003

Tseng H, Gage JA, Shen T et al (2015) A spheroid toxicity assay using magnetic 3D bioprinting and real-time mobile device-based imaging. Sci Rep 5:13987. https://doi.org/10.1038/srep13987

Wang X, Wei F, Liu A et al (2012) Biomaterials cancer stem cell labeling using poly (L-lysine)-modified iron oxide nanoparticles. Biomaterials. https://doi.org/10.1016/j.biomaterials.2012.01.058

Wang L, Huang G, Sha B et al (2014) Engineering three-dimensional cardiac microtissues for potential drug screening applications. Curr Med Chem 21:2497–2509. https://doi.org/10.2174/09298673216613121152408

Wu W, He Q, Jiang C (2008) Magnetic iron oxide nanoparticles: synthesis and surface functionalization strategies. Nanoscale Res Lett 3:397–415. https://doi.org/10.1007/s11671-008-9174-9

Wu Q, Meng N, Zhang Y et al (2014) The effect of two novel amino acid-coated magnetic nanoparticles on survival in vascular endothelial cells, bone marrow stromal cells, and macrophages. Nanoscale Res Lett 9:461. https://doi.org/10.1186/1556-276X-9-461

Wu W, Wu Z, Yu T et al (2015) Recent progress on magnetic iron oxide nanoparticles: synthesis, surface functional strategies and biomedical applications. Sci Technol Adv Mater 16:023501. https://doi.org/10.1088/1468-6996/16/2/023501

Wuest SL, Richard S, Kopp S et al (2015) Simulated microgravity: critical review on the use of random positioning machines for mammalian cell culture. Biomed Res Int. https://doi.org/10.1155/2015/971474

Zhang L, Yang G, Johnson BN, Jia X (2018) Three-dimensional (3D) printed scaffold and material selection for bone repair. Acta Biomater. https://doi.org/10.1016/j.actbio.2018.11.039